ANTICANCER RESEARCH *40*: 4947-4960 (2020)
doi:10.21873/anticanres.14498

Effects of Sclareol Against Small Cell Lung Carcinoma and the Related Mechanism: *In Vitro* and *In Vivo* Studies

HSIANG LAI CHEN[1,2], JINY YIN GONG[3], SHIH-CHAO LIN[4,5], SHIMING LI[6], YU-CHIH CHIANG[7], JUI-HSIANG HUNG[8], CHIEH-CHI YEN[9] and CHI-CHIEN LIN[2,3,10,11]

[1]*Division of Urology, Department of Surgery, Tungs' Taichung MetroHarbor Hospital, Taichung, Taiwan, R.O.C.;*
[2]*Ph.D. Program in Translational Medicine, National Chung Hsing University, Taichung, Taiwan, R.O.C.;*
[3]*Institute of Biomedical Science, The iEGG and Animal Biotechnology Center, National Chung-Hsing University, Taichung, Taiwan, R.O.C.;*
[4]*Bachelor Degree Program in Marine Biotechnology, College of Life Sciences, National Taiwan Ocean University, Keelung, Taiwan, R.O.C.;*
[5]*Department of Biomedical and Pathobiology, Virginia Polytechnic Institute and State University, Blacksburg, VA, U.S.A.;*
[6]*Hubei Key Laboratory for Processing & Application of Catalytic Materials, College of Chemistry & Chemical Engineering, Huanggang Normal University, Huanggang, P.R. China;*
[7]*Department of Restaurant, Hotel and Institutional Management, College of Human Ecology, Fu-Jen Catholic University, New Taipei City, Taiwan, R.O.C.;*
[8]*Department of Biotechnology, Chia Nan University of Pharmacy and Science, Tainan, Taiwan, R.O.C.;*
[9]*Department of Radiology, Changhua Christian Medical Foundation Changhua Christian Hospital, Changhua, Taiwan, R.O.C.;*
[10]*Department of Medical Research, China Medical University Hospital, Taichung, Taiwan, R.O.C.;*
[11]*Department of Medical Research, Taichung Veterans General Hospital, Taichung, Taiwan, R.O.C.*

Abstract. *Background/Aim: This study aimed to investigate the anticancer effects and potential mechanisms of sclareol in a human small cell lung carcinoma (SCLC) cell line. Materials and Methods: Cell viability was determined by the MTT assay. Cell cycle, apoptosis and caspase activity were evaluated by flow cytometry. Cell cycle and DNA damage related protein expression was determined by western blotting. In vivo evaluation of sclareol was carried out in xenografted tumor mice models. Results: Sclareol significantly reduced cell viability, induced G_1 phase arrest and subsequently triggered apoptosis in H1688 cells. In addition, this sclareol-induced growth arrest was associated with DNA damage as indicated by phosphorylation of H2AX, activation of ATR and Chk1. Moreover, in vivo evaluation of sclareol showed that it could inhibit tumor weight and volume in a H1688 xenograft model. Conclusion: Sclareol might be a novel and effective therapeutic agent for the treatment of SCLC patients.*

Correspondence to: Dr. Chieh-Chi Yen, Department of Radiology, Changhua Christian Medical Foundation Changhua Christian Hospital, Changhua 500, Taiwan, R.O.C. Tel: +886 47238595, e-mail: 154624@cch.org.tw; Dr. Chi-Chien Lin, Institute of Biomedical Science, National Chung Hsing University, 145 Xingda Rd., South Dist., Taichung 402, Taiwan, R.O.C. Tel: +886 422840896 ext 131, e-mail: lincc@email.nchu.nchu.edu.tw

Key Words: Small cell lung carcinoma, Sclareol, cell cycle, apoptosis, DNA damage, xenograft.

Small cell lung cancer (SCLC), previously known as oat cell carcinoma, represents 10% to 15% of all types of lung cancer cases (1). Clinically, SCLC is distinguished from non-small cell lung cancer (NSCLC) and considered as highly aggressive carcinoma because of its rapid tumor growth and early onset of metastases (2). Currently, concurrent chemoradiation (the combination of etoposide and cisplatin) remains standard treatment for early-stage SCLC (3). Another chemotherapy option is cyclophosphamide, doxorubicin, and vincristine (the CAV regimen) (4). For late-stage disease, the recommended treatment is chemotherapy alone and radiation is used for symptomatic relief (5). However, the outcome of these SCLC patients has remained stagnant over the recent decades. Most SCLC patients had disease relapse within two years and the 5-year overall survival was approximately 15% for early-stage and 5% for late-stage disease (6). Moreover, there are various chemotherapy related toxic side effects, even at usual therapeutic doses. Therefore, there is an urgent

need to identify novel, effective and safe drugs, especially from less-harmful natural sources, for the treatment of SCLC.

Sclareol [(13R)-labd-14-ene-8,13-diol], a member of the labdane-type diterpenes first purified from the Salvia sclarea plant, is abundant in nature and often used as a fragrance in cosmetics and flavoring agent in food (7). Recent studies have confirmed that sclareol exhibited anti-inflammatory and anti-tumor activity in many cancer types such as leukemia, osteosarcoma, breast cancer and colorectal carcinoma (7-10). However, to the best of our knowledge, there is no study on the role of sclareol against lung cancer. Therefore, in this study, the antitumor activities of sclareol were investigated against human SCLC cells *in vitro* and *in vivo*. In addition, the potential mechanisms involved in the anticancer effect of sclareol were investigated.

Materials and Methods

Ethics approval and consent to participate. All animal experimental procedures were carried out following the Guide for the Care and Use of Laboratory Animals of the Institutional Animal Care and Use Committee (IACUC) of the National Chung Hsing University (Taichung, Taiwan) and the procedures were approved by the Research Ethics Committee of National Chung Hsing University (approval number: IACUC 107-049).

Cell culture and materials. The human H1688 and H146 SCLC cell lines were purchased from the Food Industry Research and Development Institute (Hsinchu City, Taiwan) (11-12). These cells were cultured in RPMI 1640 supplemented with 10% fetal bovine serum and an antibiotic-antimycotic solution (containing amphotericin B, penicillin, and streptomycin). Cell culture reagents were purchased from Invitrogen Life Technologies (Carlsbad, CA, USA). The cells were incubated at 37˚C in a humidified incubator with 5% CO_2. Sclareol was dissolved in dimethylsulfoxide (DMSO) to prepare a 100 mM stock solution (Sigma-Aldrich, St. Louis, MO, USA).

Cell viability assay. The H1688 and H146 cells were seeded at a density of 4×10^4 cell/well in 24-well plates (Corning Glass Works, Corning, NY, USA). The next day, the cells were treated with 3.125 – 100 μM sclareol for 24 h. Following incubation, the medium was replaced with fresh medium containing 200 μl of 0.5 mg/ml methyl thiazolyl tetrazolium (MTT) solution (MTT, Sigma-Aldrich, St. Louis, MO, USA) for 4 h. Then, the formazan crystals were dissolved in DMSO, and the OD value at 540 nm was measured using an ELISA reader (TECAN, Durham, NC, USA). The IC_{50} was obtained by polynomial regression analysis using Microsoft Excel software, and the mean optical density (OD) ± SD for each group of triplicates was calculated.

Cell cycle assay. The H1688 cells were incubated at a density of 2×10^5 in 6-well plates. The next day, cells were treated with 25, 50 and 100 μM of sclareol for 24 h or 100 μM of sclareol for 0, 6, 12, 24 h. Following incubation, the cells were harvested by trypsin-EDTA treatment, centrifugation, and fixation with 70% ethanol at 4˚C overnight. After washing with PBS, the cells were resuspended in a propidium iodide (PI) solution containing 2 mg/ml RNase, 1 mg/ml PI and 5% Triton X-100 at RT in the dark for 30 min. Fluorescence intensity in all samples was detected and measured using an Accuri™ C5 cytometer (BD Biosciences, San Jose, CA, USA) and analyzed using BD Accuri C6 Software version 1.0.264.21.

Colony-forming assays. Cells were seeded into 6-well plates at 500 cells/well and treated with various concentrations of sclareol. After 7 days, the plates were stained with 0.5 ml of 2% crystal violet and the colonies were then counted under an inverted microscope (Olympus, Tokyo, Japan).

Annexin-FITC apoptotic assay. The H1688 cells were cultured at a density of 2×10^5 in 6-well plate (Corning Glass Works, Corning, NY, USA). The next day, the cells were treated with 100 μM of sclareol for 0, 6, 12, 24 h. Following incubation, the cells were collected by trypsin-EDTA treatment and centrifugation. Quantification of apoptotic cells was performed using an annexin V-FITC apoptosis detection kit (BD Biosciences, San Diego, CA, USA). The cells were stained according to Annexin V-FITC/PI staining protocol for 15 min at RT. Then, fluorescence of Annexin V/PI was detected with an Accuri™ C5 cytometer (BD Biosciences) and analyzed using BD Accuri C6 Software version 1.0.264.21.

Caspase activity assay. Caspase-3 activity was determined by using the CaspGLOW- fluorescein active caspase-3 staining kit (BioVision, Milpitas, CA, USA). In brief, H1688 cells were collected after treatment with 100 μM of sclareol for 0, 6, 12, 24 h. Then, the cells were rinsed with PBS and stained using CaspGLOW™ fluorescein active caspase-3 staining kit. The caspase-3 activity in the samples was quantified using an AccuriTM C5 cytometer (BD Biosciences).

ATR and Chk1 inhibitor treatment. The H1688 cells were pre-treated with BAY 1895344 (ATR Inhibitor) (Cayman Chemical, Ann Arbor, MI, USA) or AZD 7762 (chk1 inhibitor) (Cayman Chemical) for 4 h, followed by treatment with 100 μM sclareol for 12 h. Then, cells were collected by trypsin-EDTA treatment and rinsed with PBS. Cell cycle distribution and fluorescence of Annexin V/PI were evaluated by AccuriTM C5 cytometer (BD Biosciences).

Western blot. The H1688 cells were cultured at a density of 2×10^5 in 6-well plate (Corning Glass Works, Corning, NY, USA). Next day, the cells were treated with 25, 50 and 100 μM of sclareol for 24 h or 100 μM of sclareol for 0, 6, 12, 24 h. Following incubation, the cells were collected by trypsin-EDTA treatment and centrifugation. The cells were lysed in 4% SDS lysis buffer containing 1% protease inhibitor cocktail (Sigma-Aldrich) and 2% phenylmethanesulfonyl fluoride (PMSF; Sigma-Aldrich). The cell lysates were centrifuged at 13,000 × *g* for 15 min at 4˚C, and the protein concentrations in the lysates were determined using BCA Protein Assay kit (Thermo Fisher Scientific, Waltham, MA, USA). Then, the proteins were separated by SDS–PAGE and transferred onto PVDF membrane (Merck Millipore, Billerica, MA, USA). Following transfer, the membrane was blocked with a blocking buffer containing 5% non-fat milk for 1 h at room temperature and incubated with primary antibodies at 4˚C overnight. the primary antibodies were anti-cyclin D (Epitomics, Burlingame, CA, USA), anti-cyclin E (clone D7T3U) (Cell Signaling Technology, Inc., Danvers, MA, USA), anti-CDK4 (Epitomics), anti-ATR-ser-428 (Santa Cruz Biotechnology, Santa Cruz, CA, USA), anti-pATM (ser1981), anti-ATM (Santa Cruz Biotechnology), anti-phospho-CHK-1-ser-345 (Santa Cruz Biotechnology), anti-phsopho-

CHK-2-Thr68 (Santa Cruz Biotechnology) ,anti-phospho-Rb-ser-780 (GeneTex, Inc., San Antonio, TX, USA), anti-E2F1 (GeneTex), anti-phospho-Hisyone-H2A.X Ser139 (Cell Signaling Technology, Inc.,), anti- c-PARP-Asp214 (Cell Signaling Technology), and â-actin (GeneTex, Inc.). The next day, membranes were incubated with appropriate horseradish peroxidase (HRP)-conjugated secondary antibodies (Jackson ImmunoResearch Laboratories, West Grove, PA, USA) at 4˚C overnight. Finally, the enhanced chemiluminescence detection kit reagent (GE Healthcare Life Sciences, Piscataway, NJ, USA) was added for immunofluorescence signal detection using chemiluminescence (Hansor, Taichung, Taiwan). All bands in the blots were normalized to the level of â-actin. The intensity of the bands was quantified using ImageJ 1.47 software for Windows, from the National Institutes of Health (NIH) (Bethesda, MD, USA).

Animal experimentation. Six-week-old and 18-22 g weight BALB/c athymic nude female mice, were purchased from the National Laboratory Animal Center (Taipei, Taiwan) and randomly divided into two groups. Each group consisted of five mice and housed at a constant room temperature, maintained on a 12 h light/dark cycle, and fed a standard rodent diet and water. Ethical approval was obtained from the Institutional Animal Care and Use Committee (IACUC) of the National Chung Hsing University (NCHU) (approval number: IACUC 107-049). This study complied with relevant guidelines and regulations for humane animal treatment.

Tumor xenograft model. The H1688 cells (2×10^6) were suspended in 0.2 ml of extracellular matrix gel (Corning, Bedford, MA, USA) and injected subcutaneously. On the 7th day after transplantation (the tumor cell size was less than 10 mm^3), the mice were intraperitoneally injected with 300 mg/kg sclareol or the vehicle control (10% DMSO + 90% olive oil) (Sigma-Aldrich) every day until day 20. Nude mice were sacrificed on day 21 after the administration, and the tumor was excised from the nude mice, photographs of the tumors were obtained, and the tumors were weighed. The dosage and route of sclareol injection were based on previous research (13). To evaluate the toxicity of sclareol treatment in mice, the body, heart, lung, liver, kidney, and spleen weight were recorded.

Evaluation of side effects of sclareol treatment in mouse. In order to determine the side effects of sclareol on normal mice, 10 female BALB/c mice were randomly divided into the following two groups: vehicle control (n=5) and sclareol (300 mg/kg). The mice were given intraperitoneally vehicle or sclareol every day for 14 consecutive days. Mice were sacrificed on day 15 and blood was collected for side effects analysis. The blood plasma was analyzed using Neubauer's chamber, and mean numbers of red blood cells (RBC) and white blood cells (WBC) were calculated. In order to further examine the toxicity caused by the treatment with sclareol, liver function (alanine aminotransferase and alkaline phosphatase) and renal function tests (urea and creatinine) were performed.

Statistical analyses. All data are presented as mean±standard deviation (SD) of three independent experiments. An unpaired two-tailed *t*-test (Student's *t*-test) was used to compare between two groups and one-way or two-way ANOVA was used to compare multiple groups according to the experiments. A difference was considered statistically significant if *p*-value was <0.05. All data were analyzed using GraphPad Prism version 5.0 (San Diego, CA, USA).

Results

Cytotoxic effect of sclareol on the proliferation of H146 and H1688 tumor cells. The cytotoxic effect of sclareol on the viability of SCLC cell lines was determined by the MTT assay. Initially, we treated the two human SCLC cell lines (H1688 and H146) with different concentrations of sclareol for 24 h. As shown in Figure 1A, sclareol induced cytotoxicity in human SCLC cell lines in a dose-dependent manner. Notably, these two SCLC cell lines exhibited different sensitivities to sclareol; the 50% inhibitory concentration (IC_{50}) value of sclareol for H1688 cells was 42.14 μM at 24 h, while the IC_{50} value for H146 cells was 69.96 μM at 24 h, respectively. Moreover, colony formation assays showed dose-dependent inhibition of H1688 (Figure 1B and C) after 1-week treatment with sclareol, further confirming the cell growth inhibitory effect of sclareol. Because the H1688 cell line was more sensitive to sclareol treatment, we selected H1688 for further analysis and evaluation of the cytotoxic potency of sclareol.

Sclareol induced cell cycle arrest at the G_1 phase and subsequently induced cell apoptosis in H1688 tumor cells. Next, the impact of sclareol on the distribution of H1688 cells in the different cell cycle phases was evaluated. H1688 cells were exposed to different concentrations (0, 25, 50, and 100 μM) of sclareol for 24 h or were treated with 100 μM sclareol for 6, 12, and 24 h. Cellular DNA content was subjected to flow cytometric analysis after PI staining. In Figure 2A and B, the percentage of cells in the G_1 phase was significantly increased with exposure to 50 μM sclareol for 24 h. Additionally, the sub-G_1 cell population, which is indicative of cell death, was increased in the presence of 50 and 100 μM sclareol. Moreover, we also observed that the G_1 arrest caused by sclareol treatment reached its highest value at 6 h, and then at 12 and 24 h, the G_1 arrest gradually decreased, while the sub-G_1 phase gradually increased (Figure 2C and D).

To examine whether apoptotic mechanisms were involved in the cell death related to sclareol treatment, H1688 cells were treated with different concentrations and for various time periods with sclareol and subjected to flow cytometric analysis after annexin V-FITC and PI staining. A quantitative flow cytometric analysis showed that the percentages of early apoptotic (annexin V+/PI−, lower right quadrant) and late apoptotic (annexin V+/PI+, upper right quadrant) H1688 cells increased in a dose- (Figure 3A and C) and time-dependent manner (Figure 3B and D). Moreover, as shown in Figure 4, sclareol also activated caspase-3 (Figure 4A-D) and PARP expression (Figure 4F and G) in a dose- and time-dependent manner. These data suggested that sclareol promoted cell cycle arrest at the G_1 phase, and subsequently induced cell apoptosis.

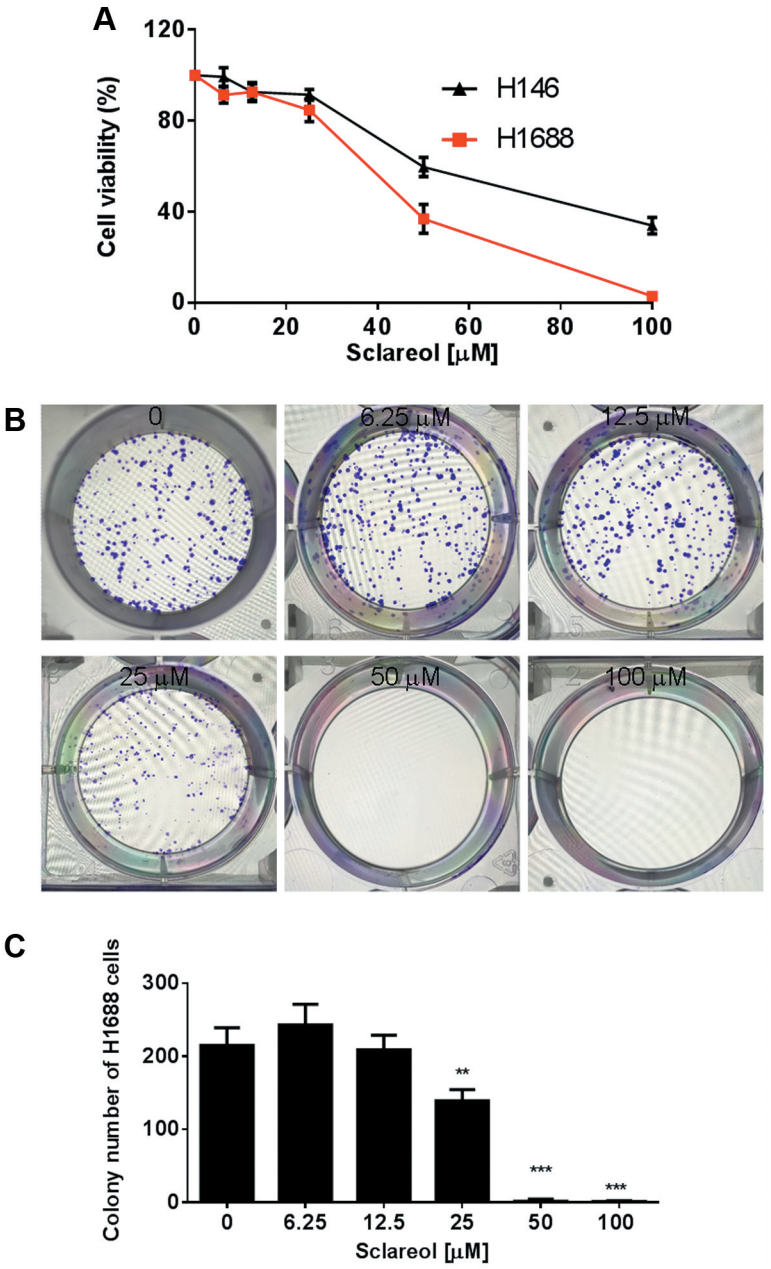

Figure 1. *Effect of sclareol on the viability and colony formation of human SCLC cancer cell lines. A: The H1688 and H146 cells were exposed to the indicated concentrations of sclareol for 24 h, and the viability of the cells was determined by the MTT assay. Cell viabilities are depicted as percentages; vehicle-treated cells were regarded as 100% viable. B: Colony formation assay of H1688 cells following treatment with sclareol for 1 week. C: The data are presented as means±SD from triplicate samples for each treatment. **p<0.01, ***p<0.001 versus DMSO-treated control (0), as determined by a one-way ANOVA with Tukey's multiple comparison test.*

Sclareol suppress G_1 phase regulatory protein levels in H1688 tumor cells. To investigate the molecular mechanisms of sclareol in the induction of G_1 phase arrest, we examined the effect of sclareol on the expression of key cell cycle regulators of G_1 phase progression. Western blotting showed that sclareol down-regulated the expression of cyclin E and D, CDK4, p-Rb (ser 780) and up-regulated the expression of E2F1, leading to G_0/G_1 phase arrest in H1688 cells and this effect was dose- and time-dependent (Figure 5).

Sclareol induced G_1 phase arrest and apoptosis through the ATR pathway in the DNA damage response. DNA damage is

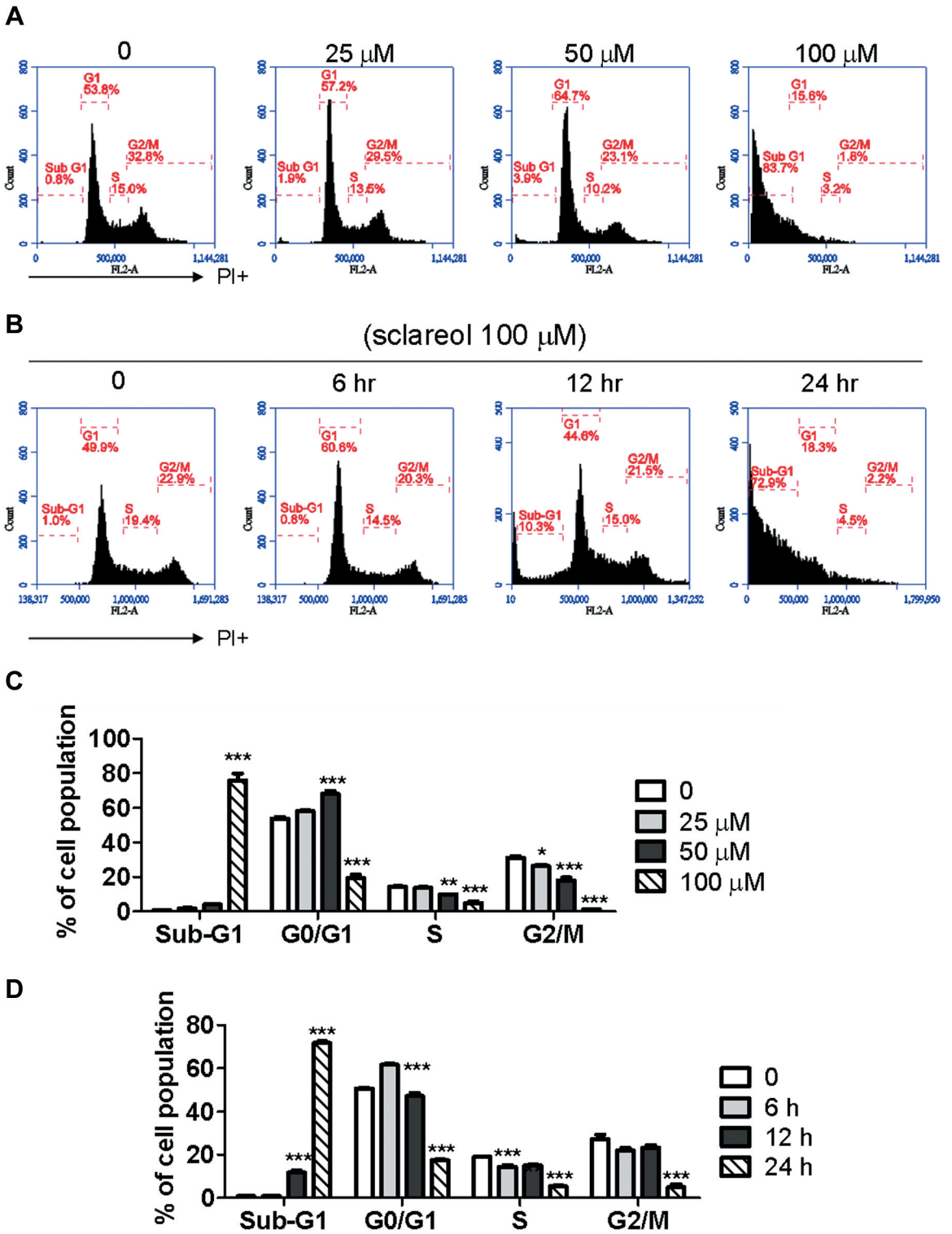

Figure 2. *Effect of sclareol on the distribution of in H1688 cells in the various phases of the cell cycle. A: Cell cycle distribution of H1688 cells after treatment with different concentrations of sclareol for 24 h. B: Cell cycle distribution of H1688 cells treated with 100 μM sclareol for 0, 6, 12, 24 h. C, D: Quantitative analysis of G_1 and Sub-G_1 proportion H1688 cells after treatment with different concentrations of sclareol for various time periods. The data are presented as means±SD from triplicate samples for each treatment. *p<0.05, ***p<0.001 versus DMSO-treated control (0), as determined by a one-way ANOVA with Tukey's multiple comparison test.*

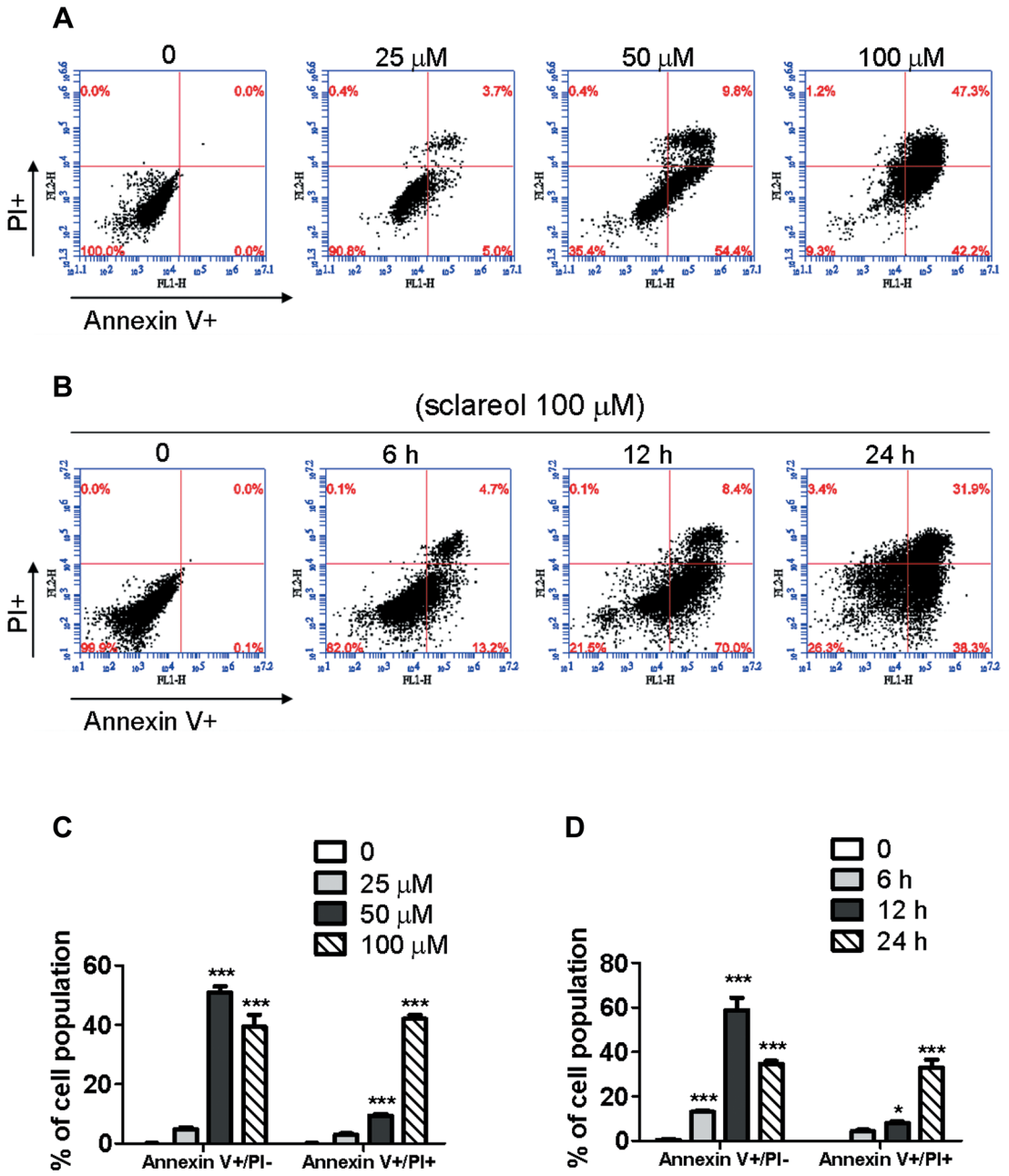

Figure 3. *Effect of sclareol on apoptosis in H1688 cells. H1688 cells were treated with different doses of sclareol for 24 h (A) or 100 μM sclareol for 0, 6, 12, 24 h (B). Cell apoptosis was examined by flow cytometry analysis of Annexin V-FITC and PI double-stained cells and (C and D) The data are presented as means±SD from triplicate samples for each treatment. *p<0.05, ***p<0.001 versus DMSO-treated control (0), as determined by a one-way ANOVA with Tukey's multiple comparison test.*

sensed by several molecular complexes or pathways, the most notable of which is the ATR/ATM that activates DNA damage response. Upon activation, ATM and ATR phosphorylate and activate the downstream effector checkpoint kinases Chk2 and Chk1, respectively. As shown in Figure 6, we observed that sclareol increased phospho-histone H2A.X Ser139 (γ-H2A.X), a known marker of DNA double-strand breaks (DSBs), p-ATR (Ser428) and p-CHK1 (Ser345) expression, whereas p-ATM (Ser1981) and p-CHK2 (Thr68) remained unchanged. Further, when H1688 cells were treated with the ATR inhibitor BAY 1895344 or the Chk1 inhibitor AZD 7762, we observed a significant

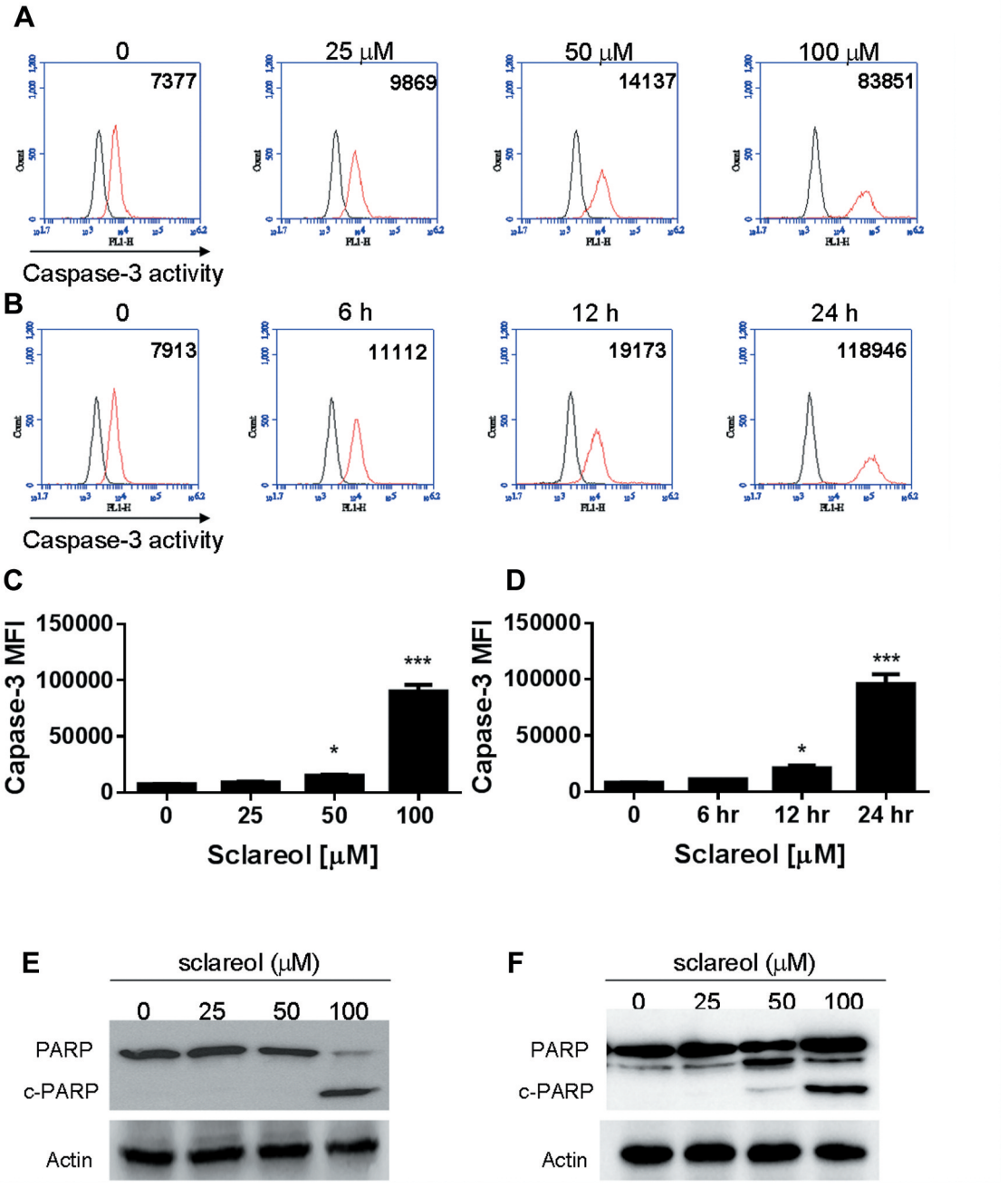

Figure 4. *Effect of sclareol on caspase -3 activity and cleaved PARP expression in H1688 cells. H1688 cells were treated with different doses of sclareol for 24 h (A) or 100 μM sclareol for 0, 6, 12, 24 h (B). The activity of caspase-3, was analyzed by flow cytometry and (C and D) The data are presented as the average of the mean fluorescence intensity (MFI) of caspase-3 activity±SD from triplicate samples for each treatment. *p<0.05, ***p<0.001 versus DMSO-treated control (0), as determined by a one-way ANOVA with Tukey's multiple comparison test. E and F: Cleaved PARP expression was measured by western blot. GAPDH was used as a loading control, and the expression levels (mean±SD, n=3) were quantified by ImageJ software and plotted in bar graphs.*

decrease in sclareol-induced cell cycle arrest (Figure 7A and B) and apoptosis (Figure 7C and D) These results imply that ATR/CHK1 activation involved in the DNA damage signaling mediates sclareol-induced G_1 arrest and apoptosis.

Sclareol inhibits H1688 tumor growth in xenograft animal model experiments. We next evaluated whether sclareol had an effect against H1688 xenografts in nude mice. On day 7, the sclareol (300 mg/kg) intraperitoneally injected mice

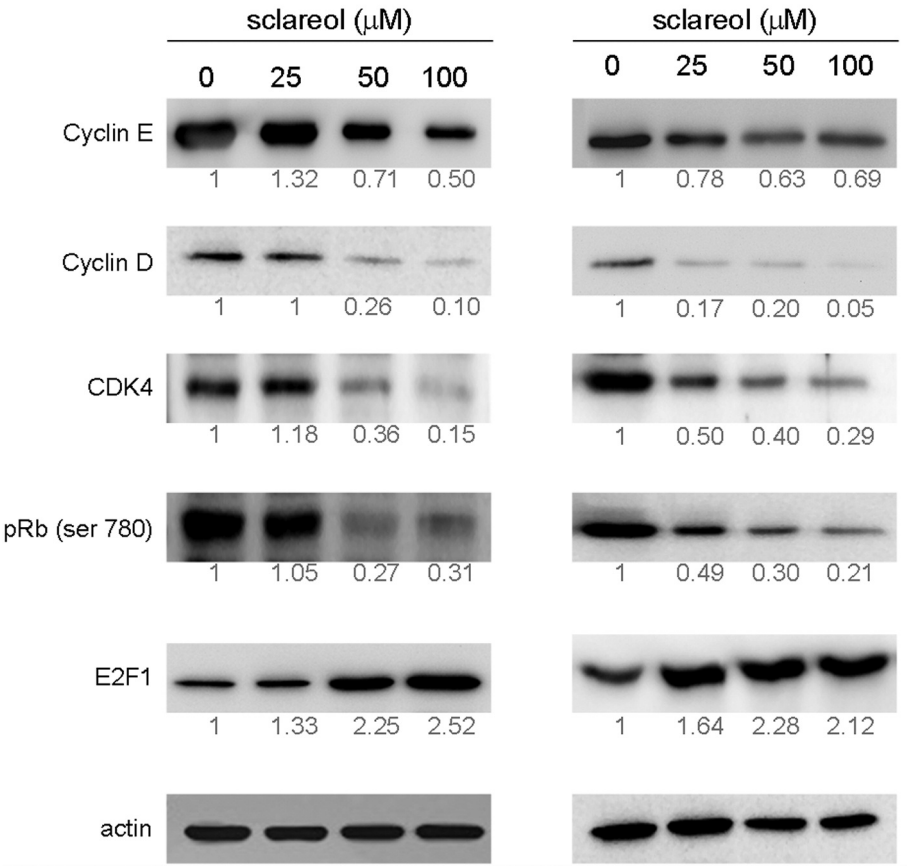

Figure 5. *Effect of sclareol on G_1 phase cell cycle related protein levels in H1688 cells. The H1688 cells were exposed to different concentrations of sclareol for 24 h or 100 μM sclareol for 0, 6, 12, 24 h. The cell lysates were prepared and expression of proteins related to the G_1 phase of cell cycle including cyclin D, cyclin E, CDK4, pRb (Ser-807/811), and E2F1 was determined by western blot. GAPDH was used as a loading control. The expression levels were quantified by ImageJ software.*

group showed a reduction in tumor growth (Figure 8A and B). Following sacrifice on day 21, the tumor size in the sclareol-treated group was significantly smaller than that in the vehicle control group. These results indicated that sclareol could suppress tumor growth *in vivo*.

In addition, we also used normal mice to further assess whether oral administration of sclareol has potential side effects (300 mg/kg body weight, 14 doses continuously; one dose/day). No significant changes in body weight (Figure 9A) and tissues weight (Heart, Liver, spleen, lung and kidney) were observed in mice treated with sclareol compared to vehicle-control mice (Figure 9B). The analysis of blood parameters of the liver and kidney functions by examining markers such as alkaline phosphatase and creatinine did not show any statistically significant difference between the two groups (Figure 9C), suggesting that oral administration with 300 mg/kg sclareol did not have significant side effects in mice.

Discussion

Although the anticancer effect of sclareol has been studied for long time, its exact role in lung cancer remains unknown. In this study, we investigated the inhibitory effect of sclareol on the human SCLC H1688 cell line and tumor growth and its potential mechanisms. Our results showed that sclareol inhibited growth of H1688 cancer cells following 24 h incubation. In addition, our results also showed that sclareol promoted G_1 phase cell cycle arrest through the ATR/CHK1 pathway involved in DNA damage response, and apoptosis. Moreover, in a SCID mouse xenograft model experiment, sclareol also showed an *in vivo* antitumor effect, and had no significant side effects in normal mice. Thus, sclareol would be a novel therapeutic agent in the treatment of human SCLC in the future.

Lung cancer remains the leading cause of cancer-related death worldwide (14). Despite early diagnosis and advances

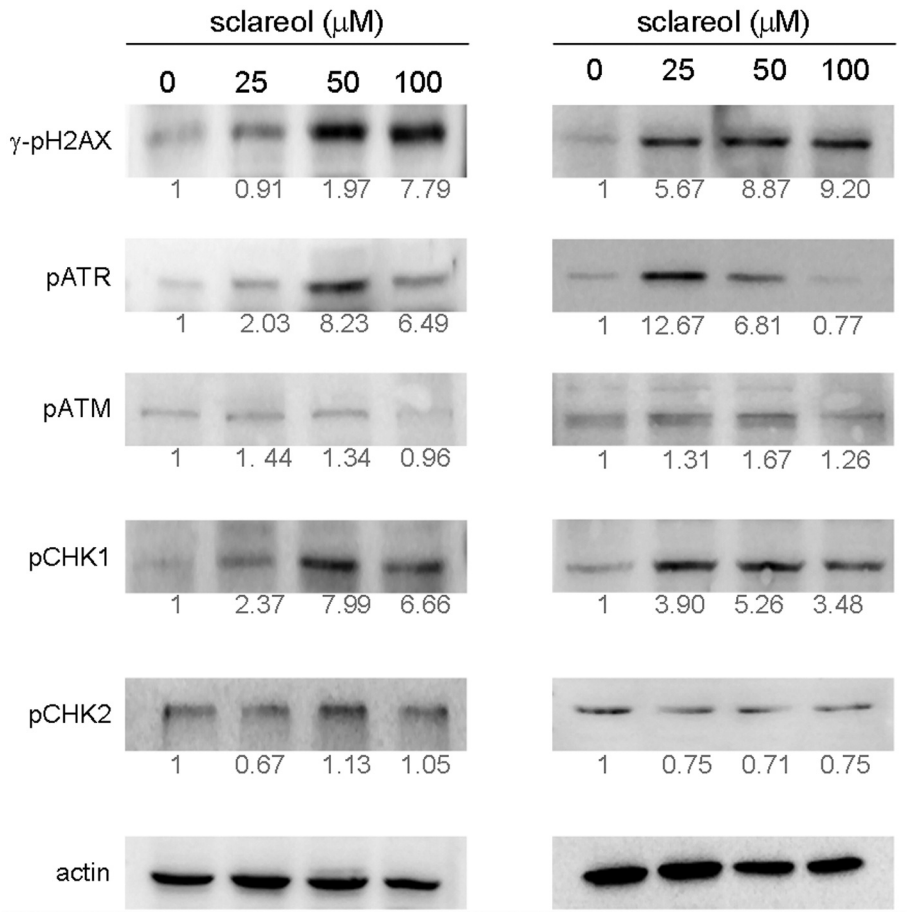

Figure 6. *Effect of sclareol on the expression levels of DNA damage-related proteins in H1688 cells. H1688 cells were exposed to 100 μM sclareol for 0, 6, 12, 24 h. The cell lysates were prepared and the expression of DNA damage-related proteins including phospho-H2A.X Ser139 (γ-H2A.X), p-ATRSer428, p-ATMser1981, p-CHK1Ser345, p-CHK2Thr68 was determined by western blot. GAPDH was used as a loading control, and protein expression levels were quantified by ImageJ software.*

in therapeutic strategies, the 5-year survival of lung cancer patients remained poor in recent decades especially for SCLC patients (15). Recurrence disease is often observed within 2 years and the main cause of treatment failure has been resistance to standard therapy (16). Further, therapy-associated side effects are major concerns of chemotherapy. Thus, it is desirable to find novel effective drugs that originate from less-harmful natural materials to replace or complement the traditional chemotherapeutics. Previous studies have reported that substances naturally occurring in foods such as fruits or vegetables may exert a chemopreventive and therapeutic effect against cancers (17, 18). As a natural labdane-type diterpene present in Salvia sclarea plant, sclareol is thought to be a potential anticancer drug because of its anti-inflammatory, and antitumor activities (7-10, 19). Although, many studies have confirmed that sclareol exhibits the hallmarks of a valuable and well-tolerated anticancer agent, thus demonstrating a greater potential for clinical applications, no study has investigated its anticancer mechanisms in SCLC.

Many recent studies have reported the antitumor effect of sclareol on various malignant cancers (7-10, 20). To our best knowledge, this study is the first to report that sclareol could also inhibit SCLC tumor growth. Although the potential mechanisms of sclareol effects are still unclear, sclareol could influence multiple signaling pathways critical to cancer development. It has been reported that sclareol could induce cell cycle arrest and apoptosis in many cancer cells, including leukemia, osteosarcoma, breast cancer and colorectal carcinoma. Our results indicated that sclareol induced cell cycle arrest at the G_1 phase through caspase-related apoptosis. The cyclin D– and E–CDK4 complexes are the most important regulators of the progression from the G_1 phase to the S phase. If the cyclin D or E complex is inhibited, cell cycle is arrested in the G_1 phase, leading to the inhibition of cell proliferation

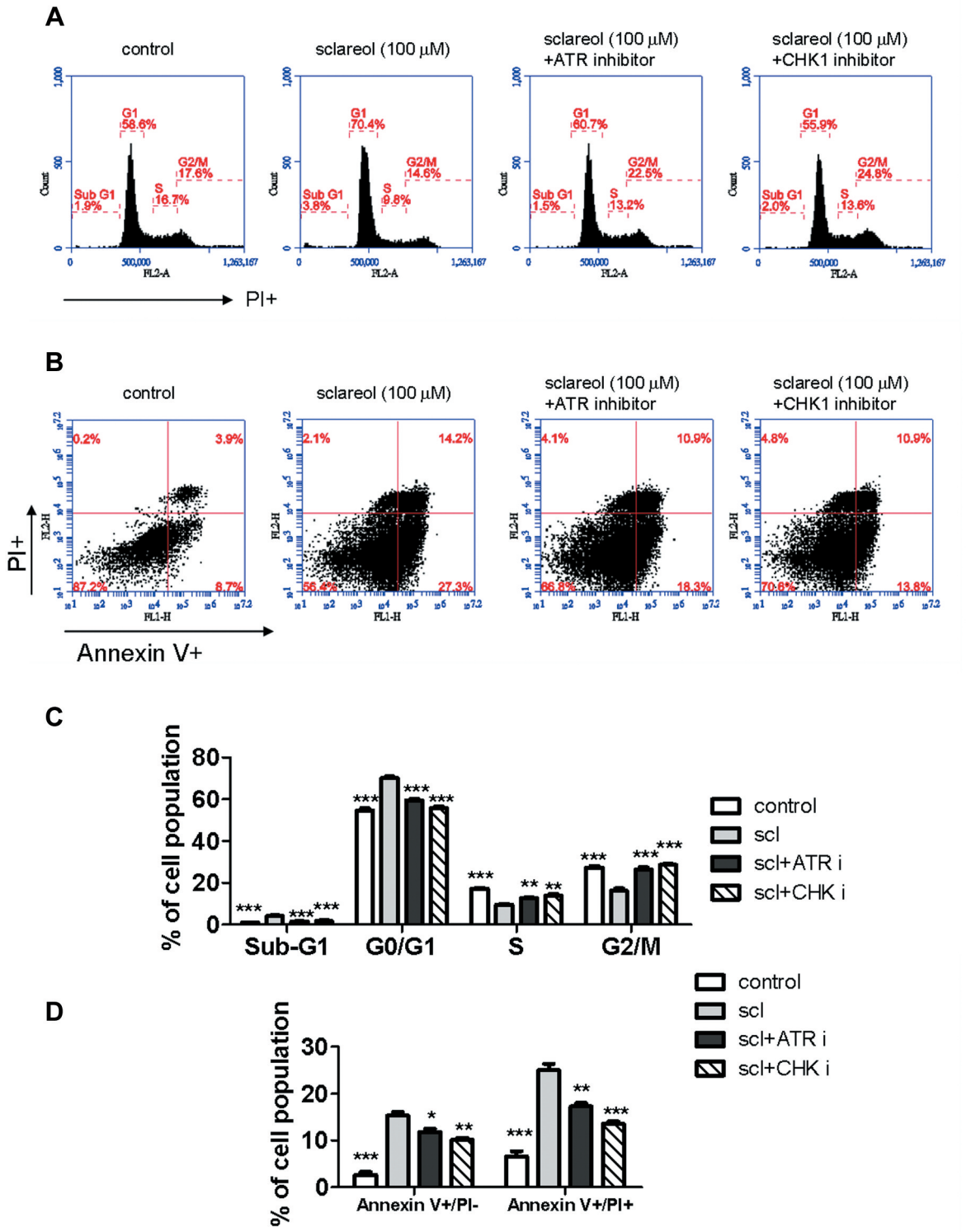

Figure 7. *Effects of the ATR inhibitor BAY 1895344 or the Chk1 inhibitor AZD 7762 on sclareol-induced cell cycle distribution and apoptosis. H1688 cells were either untreated or pretreated with 10 nM BAY 1895344 or 600 nM AZD 7762 for 4 h, followed by exposure to 100 μM sclareol. A: After 6 h, the cells were collected and stained with propidium iodide, and the DNA content was analyzed using flow cytometry. B: Cell apoptosis was examined by flow cytometry analysis of Annexin V-FITC and PI double-stained cells. C and D: Data represent the average of the cell cycle distribution±SD from triplicate samples for each treatment. *p<0.05, **p<0.01, ***p<0.001 versus 100 μM sclareol-treated control (0), as determined by a one-way ANOVA with Tukey's multiple comparison test.*

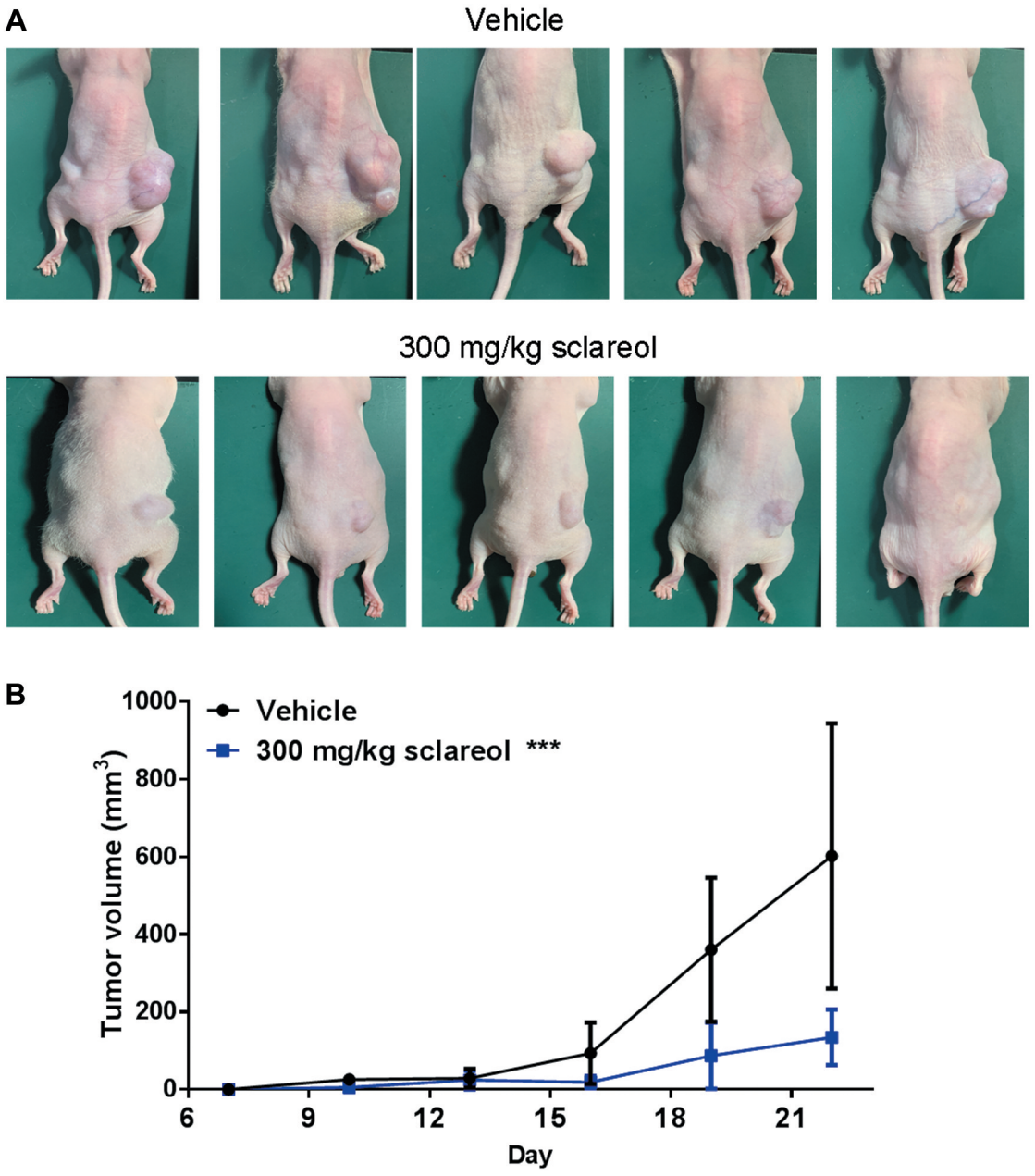

Figure 8. *Effect of sclareol on H1688 tumor growth in nude mice. H1688 cells (2×10^6) were subcutaneously injected into mice, producing a visible tumor (approximately 10 mm^3). Sclareol (300 mg/kg) or vehicle were administered intraperitoneally daily until day 21 (n=5). A: Representative images of xenograft nude mice showing regression in tumor volume after treatment with sclareol in comparison to vehicle treated group. B: The graph shows the tumor volume changes with time. Both quantified data are presented as the means±SD (n=5). ***p<0.001 versus vehicle-treated control (0), as determined by a two-way ANOVA.*

and the promotion of apoptosis. Treatment with sclareol had a marked suppressive effect on the expression of cyclin D, cyclin E and CDK4. In agreement with our results, Dimas *et al*. have also reported that sclareol induced cell cycle arrest at the G_1 phase in human HCT116 colon cancer cells (21). Moreover, the Rb protein is a tumor suppressor, and responsible for a major G_1 checkpoint, blocking S-phase entry and cell growth (22). The pRb protein represses gene transcription, required for transition from G_1 to S phase, by directly binding to the transactivation domain of E2F and by binding to the promoter of these genes as a complex with E2F. Our results indicated that sclareol can negatively regulate the cell cycle through the

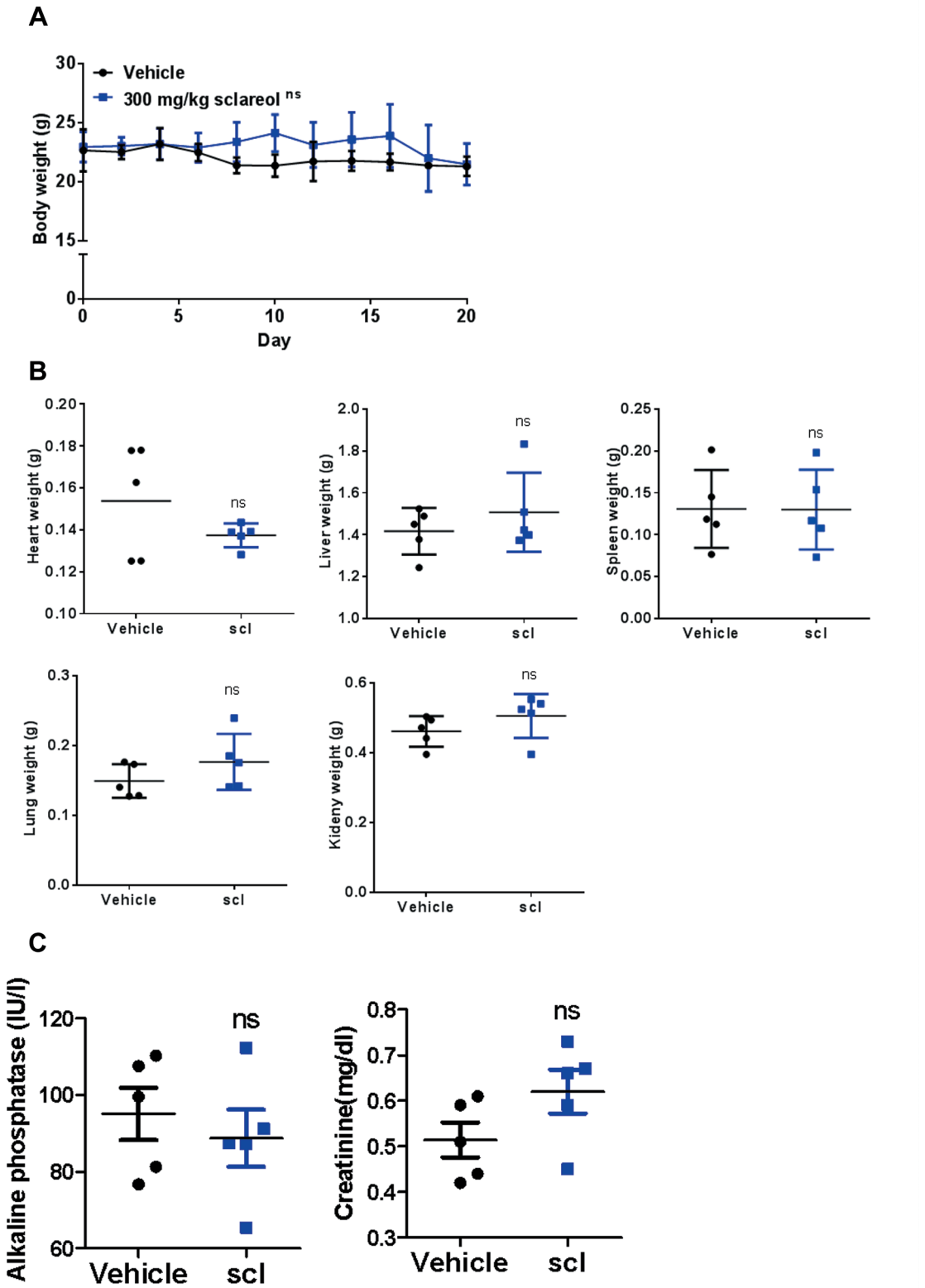

Figure 9. *Evaluation of the side effects of sclareol-treatment in mice. Mice were treated with sclareol (300mg/kg; intraperitoneally, 14 doses; one dose/day). Body weights (A) and tissues weight (B) of female BALB/c mice injected either sclareol or vehicle. C: Liver function tests (alkaline phosphatase) and kidney function tests (creatinine) were evaluated on day 15. The data are presented as means±SD (n=5). ns: p>0.05 versus vehicle-treated control, as determined by a two-way ANOVA or student t-test.*

direct decrease in the expression of phosphor-Rb protein. These findings suggested that sclareol induced G_1 phase arrest by regulating the expression of G_1 phase cell cycle regulatory proteins in H1688 cells.

A previous study had demonstrated that sclareol could induce DNA damage in human colon cancer cell lines (HCT116) and chromatin DNA breaks continued to accumulate as the cells continued to be exposed to sclareol (21). Our results showed that sclareol increased p-H2AX, p-ATR and p-Chk1 expression. Further, when H1688 cells were treated with the ATR inhibitor BAY 1895344 or the Chk1 inhibitor AZD 7762, a significant decrease in sclareol-induced G_1 arrest and annexin V positive cells was observed. These findings suggested that sclareol induced G_1 phase cell cycle arrest and apoptosis through the ATR/CHK1 pathway involved in DNA damage response in H1688 cells. However, BAY 1895344 and AZD 7762 did not fully suppress sclareol-induced G_1 arrest and apoptosis, suggesting that the involvement of other pathways cannot be ruled out. A previous study has reported that sclareol provides its anticancer effects in cervical cancer cells by enhancing the decreased expression of SOD1 *via* upregulating the tumor suppressor caveolin-1, which is involved in chaperone-mediated autophagy (CMA)-mediated protein degradation (23). Moreover, sclareol has been shown to increase the amount of endoplasmic reticulum (ER) stress in human gastric cancer cells through regulating IRE-1 and PERK genes, which are involved in ER-stress-induced apoptotic signaling (24). Furthermore, sclareol has also been shown to induce suicidal death *via* triggering phospholipid scrambling of the erythrocyte cell membrane through activation of p38 kinase and casein kinase 1α (25). These studies provide lines of experimental evidence that there are additional mechanisms in sclareol-induced cell death in NSCLC, such as autophagy or ER stress, which need to be further investigated.

In the present study, the higher dose of sclareol (300 mg/kg) was used for the comparison with previous studies; however, no significant adverse effect was found after administration. A previous study has reported that injection of 560 mg/kg of sclareol caused mice death, severe ataxia, and significant impairment in mobility in 24 h (9). Moreover, poor solubility of the lipophilic sclareol in aqueous solutions limits the amount that can be given to animals or its further application and there are side-effects concerns (21). Recently, few studies have demonstrated a strategy to improve the therapeutic index of sclareol. For example, sclareol in combination with cisplatin enhanced the cytotoxic effects of cisplatin on NSCLC (26). Moreover, 15-(4-fluorophenyl)-sclareol (SS-12), a derivative of sclareol, effectively suppressed prostate cancer tumor proliferation *in vitro* and *in vivo* (27). Although there are limitations for sclareol application due to its insolubility in aqueous phase, molecular modifications or appropriate combination therapy may be a useful strategy to improve the anti-cancer activity of sclareol, and need to be further investigated.

In summary, we demonstrated the antitumor effect of sclareol in human SCLC. We revealed that sclareol could cause cell cycle arrest, induce apoptosis of human SCLC cell lines *in vitro*, and inhibit tumor growth *in vivo* in a mouse xenograft model. Furthermore, the present and other previous *in vivo* studies have revealed that sclareol is safe for mice (19, 21, 28). Taking all of the results into consideration, sclareol may be developed as a possible anticancer drug for the treatment of SCLC because it is a natural compound that exhibits low toxicity. Further study is needed to evaluate the efficacy of sclareol in combination with traditional chemotherapeutic regimens or radiation for SCLC.

Conflicts of Interest

The Authors declare that they have no competing interests regarding this study.

Authors' Contributions

S.-L.C., C.-C.Y. and C.-C.L conceived and designed the experiments. S.-C.L. and Y.-C.C performed the experiments. S.L. and J.-H.H analyzed the data. C.-C.Y. and C.-C.L wrote the manuscript. All Authors read and approved the final manuscript.

Acknowledgements

This study was financially supported by the iEGG and Animal Biotechnology Center from The Feature Areas Research Center Program within the framework of the Higher Education Sprout Project by the Ministry of Education (MOE-107-S-0023-E) in Taiwan, and TCVGH-108-7313C from the Taichung Veterans General Hospital.

References

1 Siegel RL, Miller KD and Jemal A: Cancer Statistics, 2017. CA Cancer J Clin *67(1)*: 7-30, 2017. PMID: 28055103. DOI: 10.3322/caac.21387

2 Caprario LC, Kent DM and Strauss GM: Effects of chemotherapy on survival of elderly patients with small-cell lung cancer: analysis of the SEER-medicare database. J Thorac Oncol *8(10)*: 1272-1281, 2013. PMID: 24457238. DOI: 10.1097/JTO.0b013e3182a007ba

3 Watkins JM, Wahlquist AE, Zauls AJ, Shirai K, Garrett-Mayer E, Aguero EG, Silvestri GA, Sherman CA and Sharma AK: Involved-field radiotherapy with concurrent chemotherapy for limited-stage small-cell lung cancer: disease control, patterns of failure and survival. J Med Imaging Radiat Oncol *54(5)*: 483-489, 2010. PMID: 20958948. DOI: 10.1111/j.1754-9485.2010.02201.x

4 Johnson BE, Bridges JD, Sobczeck M, Gray J, Linnoila RI, Gazdar AF, L Hankins, Steinberg SM, Edison M, Frame JN, Pass H, Nesbitt J, Holden D, Mulshine JL, Glatstein E and Ihde DC: Patients with limited-stage small-cell lung cancer treated with concurrent twice-daily chest radiotherapy and etoposide/cisplatin followed by cyclophosphamide, doxorubicin, and vincristine. J Clin Oncol *14(3)*: 806-813, 1996. PMID: 8622028. DOI: 10.1200/JCO.1996.14.3.806

5 Foster NR, Renfro LA, Schild SE, Redman MW, Wang XF, Dahlberg SE, Ding K, Bradbury PA, Ramalingam SS, Gandara DR, Shibata T, Saijo N, Vokes EE, Adjei AA and Mandrekar SJ: Multitrial evaluation of progression-free survival as a surrogate end point for overall survival in first-line extensive-stage small-cell lung cancer. J Thorac Oncol *10(7)*: 1099-1106, 2015. PMID: 26134227. DOI: 10.1097/JTO.0000000000000548

6 Zhu H, Guo H, Li M, Zhang Y, Han A, Shi F, Kong L and Yu J: Increased serum carcinoembryonic antigen level can predict poor survival of patients with small cell lung cancer. Transl Res *166(4)*: 355-365, 2015. PMID: 25936590. DOI: 10.1016/j.trsl.2015.04.005

7 Dimas K, Kokkinopoulos D, Demetzos C, Vaos B, Marselos M, Malamas M and Tzavaras T: The effect of sclareol on growth and cell cycle progression of human leukemic cell lines. Leuk Res *23(3)*: 217-234, 1999. PMID: 10071073. DOI: 10.1016/s0145-2126(98)00134-9

8 Wang L, He HS, Yu HL, Zeng Y, Han H, He N, Liu zg, Wanf ZY, Xu SJ and Xiong M: Sclareol, a plant diterpene, exhibits potent antiproliferative effects *via* the induction of apoptosis and mitochondrial membrane potential loss in osteosarcoma cancer cells. Mol Med Rep *11(6)*: 4273-4278, 2015. PMID: 25672419. DOI: 10.3892/mmr.2015.3325

9 Hatziantoniou S, Dimas K, Georgopoulos A, Sotiriadou N and Demetzos C: Cytotoxic and antitumor activity of liposome-incorporated sclareol against cancer cell lines and human colon cancer xenografts. Pharmacol Res *53(1)*: 80-87, 2006. PMID: 16253514. DOI: 10.1016/j.phrs.2005.09.008

10 Dimas K, Papadaki M, Tsimplouli C, Hatziantoniou S, Alevizopoulos K, Pantazis P and Demetzos C: Labd-14-ene-8,13-diol (sclareol) induces cell cycle arrest and apoptosis in human breast cancer cells and enhances the activity of anticancer drugs. Biomed Pharmacother *60(3)*: 127-33, 2006. PMID: 16527443. DOI: 10.1016/j.biopha.2006.01.003

11 Fang C, Zhang J, Qi D, Fan X, Luo J, Liu L and Tan Q: Evodiamine induces G2/M arrest and apoptosis *via* mitochondrial and endoplasmic reticulum pathways in H446 and H1688 human small-cell lung cancer cells. PLoS One *9(12)*: e115204, 2014. PMID: 25506932. DOI: 10.1371/journal.pone.0115204

12 Matsui J, Yamamoto Y, Funahashi Y, Tsuruoka A, Watanabe T, Wakabayashi T, Uenaka T and Asada M: E7080, a novel inhibitor that targets multiple kinases, has potent antitumor activities against stem cell factor producing human small cell lung cancer H146, based on angiogenesis inhibition. Int J Cancer *122(3)*: 664-671, 2008. PMID: 17943726. DOI: 10.1002/ijc.23131

13 Li K, Dias SJ, Rimando AM, Dhar S, Mizuno CS, Penman AD, Lewin JR and Levenson AS: Pterostilbene acts through metastasis-associated protein 1 to inhibit tumor growth, progression and metastasis in prostate cancer. PLoS One *8(3)*: e57542, 2013. PMID: 17943726. DOI: 10.1371/journal.pone.0057542

14 Siegel R, Ma J, Zou Z and Jemal A: Cancer statistics, 2014. CA Cancer J Clin *64(1)*: 9-29, 2014. PMID: 24399786. DOI: 10.3322/caac.21208

15 Wang BY, Huang JY, Cheng CY, Lin CH, Ko J and Liaw YP: Lung cancer and prognosis in taiwan: a population-based cancer registry. J Thorac Oncol *8(9)*: 1128-1135, 2013. PMID: 23945383. DOI: 10.1097/JTO.0b013e31829ceba4

16 Kim ES: Chemotherapy resistance in lung cancer. Adv Exp Med Biol *893*: 189-209, 2016. PMID: 26667345. DOI: 10.1007/978-3-319-24223-1_10

17 Siddiqui IA, Adhami VM, Ahmad N and Mukhtar H: Nanochemoprevention: sustained release of bioactive food components for cancer prevention. Nutr Cancer *62(7)*: 883-890, 2010. PMID: 20924964. DOI: 10.1080/01635581.2010.509537

18 Riboli E, Slimani N and Kaaks R: Identifiability of food components for cancer chemoprevention. IARC Sci Publ *(139)*: 23-31, 1996. PMID: 8923017.

19 Noori S, Hassan ZM, Mohammadi M, Habibi Z, Sohrabi N and Bayanolhagh S: Sclareol modulates the Treg intra-tumoral infiltrated cell and inhibits tumor growth *in vivo*. Cell Immunol *263(2)*: 148-153, 2010. PMID: 20409537. DOI: 10.1016/j.cellimm.2010.02.009

20 Sashidhara KV, Rosaiah JN, Kumar A, Bid HK, Konwar R and Chattopadhyay N: Cell growth inhibitory action of an unusual labdane diterpene, 13-epi-sclareol in breast and uterine cancers *in vitro*. Phytother Res *21(11)*: 1105-1108, 2007. PMID: 17639552. DOI: 10.1002/ptr.2205

21 Dimas K, Hatziantoniou S, Tseleni S, Khan H, Georgopoulos A, Alevizopoulos K, Wyche JH, Pantazis P and Demetzos C: Sclareol induces apoptosis in human HCT116 colon cancer cells *in vitro* and suppression of HCT116 tumor growth in immunodeficient mice. Apoptosis *12(4)*: 685-694, 2007. PMID: 17260186. DOI: 10.1007/s10495-006-0026-8

22 Giacinti C and Giordano A: RB and cell cycle progression. Oncogene *25(38)*: 5220-5227, 2006. PMID: 16936740. DOI: 10.1038/sj.onc.1209615

23 Zhang T, Wang T and Cai P: Sclareol inhibits cell proliferation and sensitizes cells to the antiproliferative effect of bortezomib *via* upregulating the tumor suppressor caveolin-1 in cervical cancer cells. Mol Med Rep *15(6)*: 3566-3574, 2017. PMID: 28440485. DOI: 10.3892/mmr.2017.6480

24 Aboutalebi E, Sakhinia E, Beilanokhi V and Dolatkhah H: Investigating the effect of Sclareol on IRE-1 and PERK genes the pathway of reticulandaplasmic system stress in gastric cancer cells MKN-45. Int J Res Appl Basic Med Sci *6(1)*: 32-44, 2020. PMID: 28440485.

25 Signoretto E, Laufer SA and Lang F: Stimulating effect of sclareol on suicidal death of human erythrocytes. Cell Physiol Biochem *39(2)*: 554-564, 2016. PMID: 27395049. DOI: 10.1159/000445647

26 Li W, Ping Z, Xuemei G, Minglian L, Hongjuan M, Yi H and Zhu Z: Naturally occurring sclareol diterpene augments the chemosensitivity of human hela cervical cancer cells by inducing mitochondrial mediated programmed cell death, S-phase cell cycle arrest and targeting mitogen-activated protein kinase (MAPK)/Extracellular-signal- regulated kinase (ERK) signaling pathway. Med Sci Monit *26*: e920248, 2020. PMID: 31935210. DOI: 10.12659/MSM.920248

27 Shakeel-u-Rehman, Rah B, Lone SH, Rasool RU, Farooq S, Nayak D, Chikan NA, Chakraborty S, Behl A, Mondhe DM, Goswami A and Bhat KA: Design and synthesis of antitumor heck-coupled sclareol analogues: modulation of BH3 family members by SS-12 in autophagy and apoptotic cell death. J Med Chem *58(8)*: 3432-3444, 2015. PMID: 25825934. DOI: 10.1021/jm501942m

28 Noori S, Hassan ZM and Salehian O: Sclareol reduces CD4+ CD25+ FoxP3+ Treg cells in a breast cancer model *in vivo*. Iran J Immunol *10*: 10-21, 2013. PMID: 23502334.

Received June 10, 2020
Revised July 6, 2020
Accepted July 8, 2020